NUMERICAL SIMULATION OF NEWTONIAN FLUID MIXING INSIDE ASYMETRIC T-SHAPED MICROMIXERS

Tiago António
tiago.antonio@tecnico.ulisboa.pt

Instituto Superior Técnico, Universidade de Lisboa, Portugal

June 2019

ABSTRACT

Achieving eficient mixing of flow streams is one of the important challenges of microfluidics, because of the difficulty to induce flow transition to the turbulent regime. Of the different solutions for devices proposed, T-shaped micromixers stand out, as they have a simple geometry and low production cost and showed promising results when asymmetric inlet conditions are applied. Starting from experimental results obtained when equal flow rates were applied to inlets with different widths, four geometries (one symmetric and three asymmetric) were modelled using CAD 3D software Solidworks. Then, the numerical simulation of twelve flows, corresponding to the Reynolds number based on the outlet channel range of 25 to 295, inside each model was performed. This tool allowed the understanding of how the degree of asymmetry influence mixing quality, and the physical characterization of the five flow regimes previously identified. This allowed to conclude that increasing asymmetry favours mixing quality and also that after transition to *engulfment* regime, symmetrical micromixers perform better than asymmetrical ones.

Keywords: Microfluids; T-shaped Micromixers; Mixing; Numerical Simulation

1. Introduction

In the 90's of the preceding century, the advent of LOC (lab-on-a-chip) and μ-TAS (micro-total analysis systems) devices led to significant developments in chemical, biological and biochemical experiments in microchips, with high waste reduction, and reduced energy consumption and costs, but with the inherent scale reduction problems associated to the flows at low Reynolds numbers.

The large mixing times and lengths required for fluids mixing to occur at the scale of those devices focused the scientists attention towards the development of new chip designs, commonly named as micromixers, capable of achieving better mixing. In fact, one of the major challenges to ensure an efficient operation of some microfluidic devices in the present days is their capability of promoting mixing between fluids proficiently, due to the strong dominance of surface effects over inertial ones because of the micrometric characteristic length. These viscous effects make considerably difficult the departure from the laminar flow regime that is characterized by poor mixing capabilities [1].

A common classification of micromixers is based on the use (or not) of external energy sources to promote mixing [2,3]. According to this, one can find active and passive micromixers, the latter operating without any kind of energy inputs [2,3]. In turn, active micromixers exhibit an improved mixing quality due to the use of external energy sources, which introduce vorticity in the laminar flow, thereby enhancing molecular diffusion [1]. Although active micromixers are capable of very efficient mixing, their use poses some running costs issues and manufacture challenges as the need for an external energy source may give birth to complex geometry designs [1].

Passive micromixers, in turn, are designed to promote a mixing enhancement through the geometrical configuration of the microchannels, the only external energy source present being that of the pumps that drive the flows into the chip. Generally, their geometry should maximize the contact area between the fluids, in order to increase the molecular diffusion. It should also promote local disruptions of the deterministic flow structure so that advection, almost absent in pure laminar regime, is strengthened [4].

To promote advection, there are different geometrical solutions that potentiate the appearance of non-deterministic flow structures, like vortices. These structures exhibit cross-flow velocity components that, complementary to the advection promotion, also twist and curl the fluids interface, increasing the area of contact between the fluids and, therefore, enhancing molecular diffusion [4].

Different designs for micromixers, aiming at improving mixing through advection have been proposed [1,4]. Among these, the one that stands out is the T-micromixer. Two fluids, coming from different inlets, meet in the same mixing channel. Beyond a critical Reynolds number, the interface between both fluids begins to twist and curl and is eventually disrupted, causing advective mixing related to the centrifugal forces [5,6]. The simple design of T-micromixers makes their production easy, cheap and fast. In addition, having only two inlets and one outlet makes the T-micromixer easy to integrate into μ-TAS systems [7-9]. Moreover, compared to other solutions, friction losses along the walls are minimized, which saves pumping power [8]. This is probably why this type of micromixers has been largely studied in the literature.

Experimental and numerical studies have identified the three following different regimes for steady-state laminar flows (Reynolds numbers below 300) inside symmetrical T-micromixers [2,3,8,10]:

i) Stratified regime - This regime exists for very low Reynolds numbers and is characterized by the existence of two practically parallel unmixed streams of both fluid that flow side by side in the mixing channel. The advective mass transfer is negligible [10], the only mixing mechanism being molecular diffusion.

ii) Laminar vortex regime - For intermediate Reynolds numbers, this regime is set in and secondary flow structures appear close to the T-junction zone due to centrifugal forces. Usually, a double vortex pair is observed, but the vertical plane of symmetry in the outlet channel is preserved. These secondary flow patterns cause a slight increase in the mixing quality [10].

iii) Engulfment regime - Transition to the engulfment regime occurs at relatively high Reynolds numbers. This flow regime is characterized by the development of fine lamellae leading to a significant decrease in diffusion lengths. Rapid mixing is driven by secondary flow structures like vortices, as well as by boundary layer separation at the corners of the inlet channels [10].

As done herein, the Reynolds number, Re_{D_h}, is usually defined by using the hydraulic diameter of the outlet microchannel as the characteristic length, D_h, i.e. $Re_{D_h} = \frac{2Q\rho}{(H+W)\mu}$, with $D_h = \frac{2HW}{H+W}$. In these equations, Q is the volumetric flow rate, ρ the fluid density, μ the dynamic viscosity of the fluid and H and W are the outlet microchannel height and width, respectively.

In an effort to improve the performance of the T-micromixers, some authors performed experimental work imposing asymmetrical flow conditions at the micromixer inlets, namely asymmetry in fluids viscosity [11], in the mass flow rate [3] and, more recently, geometrical asymmetry [7,8]. The underlying idea of these attempts has been the generation of disturbing flow structures capable of promoting the disruption of the fluids interface in the outlet microchannel and, therefore, enhancing advection.

In two experimental research works [7,8], T-shaped micromixers aligned vertically and horizontally were used, but with different widths for the inlet channels. A flow of water was imposed at one inlet, and flow of a much diluted solution of bromothymol was imposed at the other. The experiments covered Reynold numbers (based on the hydraulic diameter of the mixing microchannel) in a vast range, from 50 to 310. Observations have shown five different flow regimes that are described below.

For regime I, at Re between 57 and 76, the flow is completely segregated, *i.e.* the inlet streams do not interfere with each other and a well-defined interface between both fluids is clearly visible. Molecular diffusion is the only mass transfer mechanism for the mixing process in this case [8]. For flows with Re between 95 and 133, regime II occurs and is characterized by the appearance of a residual advective mixing. The line defining the interface close to the T-junction deviates from the horizontal symmetry axis, which means that the bromothymol solution, entering into the system through the wider inlet, penetrates the water side. As a result, advection begins to play a pale role in the mixing process [8]. Regime III occurs at Re between 143 and 172. For this regime, there is some bromothymol appearing close to the channel side wall in the water side due to a local disruption of the interface separating both fluids [8]. Regime IV, occurring at Re between 229 and 267, is characterized by the complete disruption of the interface that separates both fluids, which greatly enhances the mixing quality [8] as advection is now playing an important role. Regime V, which occurs at Re above 267, is characterized by the generation of multiple vortices inside the mixing channel. The similarities of this regime with that of engulfment occurring within the symmetrical micromixer are clear. In addition, the flow also exhibits alternating layers of water and bromothymol solution superimposed, advection being the most important mechanism of mass transport for the mixing process [8].

The outcome of those research works [7,8] shows that increasing the level of geometrical asymmetry between the two inlets of the micromixer promotes the mixing quality enhancement. The critical Reynolds number values for transition between the above-described regimes where advection plays a major role decreases, allowing for a faster and more efficient mixing, even at lower Reynolds numbers.

Channel	$W_{ia}(\mu m)$	$W_{ib}(\mu m)$	$W_0(\mu m)$	$\frac{W_{ia}}{W_{ib}}$	L_0(mm)	H (μm)	$D_{h0}(\mu m)$	N_c
S1	100.31	100.31	200.63	1.00	3.00	100.94	134.30	1181568
A1	104.88	154.69	203.44	0.68	3.00	99.38	133.53	1213824
A2	102.19	175.31	200.63	0.58	3.00	99.38	132.91	1225920
A3	106.81	200.63	200.63	0.53	3.00	100.94	134.30	1246080

Table 1 Geometrical Characteristics of the geometries modelled. Nc represents the number of computational cells of a given model

Despite the promising results obtained by those works, they were very limited in providing a detailed characterization of the studied flows, mainly due to the experimental techniques restrictions related to the inherent two-dimensional microscope images acquired during the experiments. The present work addresses this issue, covering the gap of the detailed flow characterization, by taking advantage of the use of CFD to perform a detailed three-dimensional analysis of the flows inside T-micromixers and identify the physical mechanisms at stake. This brings some new insight about the influence of the asymmetry between inlets on the performance of T-micromixers. Moreover, the physical effects of increasing the Reynolds number becomes effectively clearer and consists of inducing the generation, or dissipation, of physical flow structures, namely vortices, that define specific flow mixing characteristics of the five different regimes identified.

2. Characterization of the Mixing Quality

To evaluate the performance of a micromixer, the definition of a parameter that quantifies the mixing quality achieved in such a device is mandatory. The most commonly used parameter takes into consideration the amplitude of the variations in species concentration at a defined section of the outlet channel. This parameter is the mixing quality α_{mix}, suggested by Danckwerts, and defined as expressed by equation (1) [10], with c_i being the species concentration at location *i*, *N* the total number of locations where the species concentration is known, and $c = 0.5$ is the species concentration for a homogeneous mixture. The value of α_{mix} varies between 0 and 1, with $\alpha_{mix} = 0$ corresponding to a system completely segregated and $\alpha_{mix} = 1$ to a homogeneous mixing.

$$\alpha_{mix} = 1 - \frac{\sqrt{\sum_{i=1}^{N}(c_i - 0.5)^2}}{0.5\sqrt{N}}, \qquad (1)$$

It is worth to emphasise that this work introduces a new approach to evaluate the effects of the asymmetry of the inlet conditions of the micromixers on the mixing quality (characterized by the parameter α_{mix}). In fact, the usually used independent variable (Reynolds number at the outlet channel) to quantify the mixing quality [7,8,10] is certainly unresponsive to the asymmetric flow conditions at the inlet microchannels, *i.e.* one may have exactly the same Reynolds number value for an infinite number of combinations of different inlet flow rates.

In the search for a parameter capable of accounting simultaneously for the increase of the Reynolds number (that is essential to identify the flow regimes above-described), and for the asymmetry of the device and/or inlet conditions, the choice was to use the total transported kinetic energy rate at both inlets. Being a quantity transported by the fluid elements, this parameter is calculated from equation (2), where $\vec{v}$ is the velocity vector (with a magnitude of v) and $\vec{n}$ is the normal to the surface element *dA* that refers to both inlet microchannels cross-section areas *SC*.

$$I_{KE} = \int_{SC} \frac{\rho v^2}{2}(\vec{v} \cdot \vec{n})dA \qquad (2)$$

3. Modelling

3.1 The studied micromixers geometries

The T-shaped micromixers studied herein are of the passive type. A scheme of such devices is displayed in figure 1. As it can be seen, two fluids, coming from different opposing inlets, meet in the T-junction zone and flow out through a unique mixing (or outlet) channel.

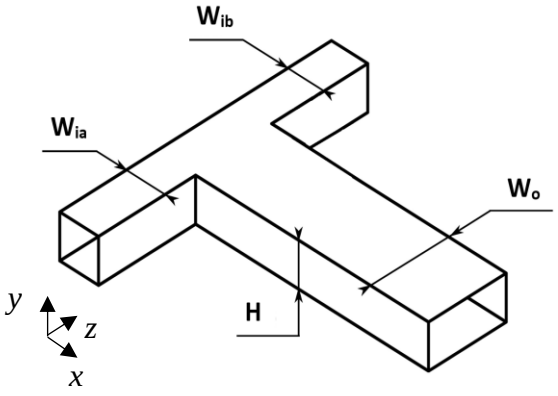

Figure 1 Representation of a T-micromixer of dimensions $W_i \times W_o \times H$

The geometrical details (characteristic dimensions and number of computational cells inside the physical domain used in the numerical simulations) are displayed in table 1. From the geometrical point of view, all micromixers have the same height. Moreover, both symmetrical (S1, with the inlet microchannels possessing the same widths) and asymmetrical (A1, the least asymmetrical one

with a ratio of the inlet microchannels widths of 0.68; A2, the one with the intermediate ratio of the inlet microchannels widths of 0.58; and A3, the most asymmetrical one with a ratio of the inlet microchannels widths of 0.53) T-micromixers are studied.

3.2 Physical and mathematical modelling

The laminar flows studied herein occur all inside T-micromixers, with both symmetrical and asymmetrical inlet conditions, and cover all the different regimes described before.

Such flows, when isothermal, are governed by the continuity equation (3) and by the Navier-Stokes equations (4), which can be written in Cartesian coordinates as follows [12].

$$\frac{\partial \rho}{\partial t} + \frac{\partial}{\partial x_i}(\rho u_i) = 0 \qquad (3)$$

$$\frac{\partial (\rho u_i)}{\partial t} + \frac{\partial}{\partial x_j}\left(\rho u_i u_j\right) = -\frac{\partial p}{\partial x_i} + \frac{\partial \tau_{ij}}{\partial x_j} + S_i \qquad (4)$$

In the previous equations, x_i is the spatial coordinate in the *i*-direction, *t* is time, u_i is the fluid velocity component in the *i*-direction, ρ is the fluid density, p is the pressure and τ_{ij} is the viscous shear stress tensor The term S_i is a mass-distributed source, representing an external force per unit volume, and gathers three different possible contributions (*i.e.* $S_i = S_i^{Porous} + S_i^{Gravity} + S_i^{Noninertial}$): i) a porous media resistance (S_i^{Porous}) – nil in the present case; ii) a volumetric force due to gravity ($S_i^{gravity} = \rho g_i$, where g_i is the gravitational acceleration component along the *i*-direction) – nil in the present case and, iii) non-inertial effects if the coordinate system is accelerating ($S_i^{Noninertial}$) – nill in the present case.

For Newtonian fluids, and considering the Kronecker delta δ_{ij}, the viscous shear stress is defined by equation (5) [19].

$$\tau_{ij} = \mu\left(\frac{\partial u_i}{\partial x_j} + \frac{\partial u_j}{\partial x_i} - \frac{2}{3}\delta_{ij}\frac{\partial u_k}{\partial x_k}\right) \qquad (5)$$

In addition to the previous equations (3-5), the advection-diffusion transport equation for species-*m* mass concentration, y_m, has also to be solved whenever two fluids mixture occurs as in this case, which runs [19]:

$$\frac{\partial (\rho y_m)}{\partial t} + \frac{\partial}{\partial x_i}(\rho u_i y_m) = \frac{\partial}{\partial x_i}\left(D_{mn}\frac{\partial y_n}{\partial x_i}\right) + S_m \qquad (6)$$

In the previous equation, D_{mn} is the molecular mass diffusivity tensor and S_m is the rate of production or consumption of the *m*-species. Applying the Fick's diffusion law, the diffusivity tensor may be calculated from $D_{mn} = D\delta_{nm}$, where D is a molecular diffusivity and δ_{nm} is the Kronecker delta.

Since we are in the presence of an ideal binary solution after the occurrence of the mixing of two fluids, the mass concentration of the other species, species-*n*, y_n, is promptly obtained from $y_n = 1 - y_m$.

The previous equations are numerically solved by using the commercial software *Solidworks Flow Simulation 2017*. This choice was made due to the availability of a license and the fact that its graphical interface is quite user-friendly. It should be noted that the numerical technique of that software treats all problems as time-dependent and, therefore, for steady-state problems the simulation stops once the variables values stabilize in time and meet the spatial convergence criteria.

Solidworks Flow Simulation uses a fully implicit variation the *Cell Centred Finite Volume Method* with Cartesian coordinates. Moreover, diffusive terms are computed at the centre of each cell face using a *Central Difference Scheme* (CDS), and the convective terms are computed at the same location and use an *Upwind Differencing Scheme* (UDS) [12]. Pressure and velocity coupling is performed with the SIMPLER algorithm [13].

To compare the numerical solutions with the corresponding experimental results obtained in a previous research work [10], four CAD geometries (S1, A1, A2 and A3 as displayed in table 1) with the same dimensions as those of the experiments were generated. Both inlets and outlets were designed long enough to ensure that the results are independent from these parameters.

Using the grid generation software, the respective meshes for each geometry were generated – see illustrative scheme in figure 2. Preliminary simulations showed strong concentration gradients at the T-junction region and along the mixing channel. Therefore, since uniform meshes were used, the refinement was concentrated in those regions. Cells were chosen to be mainly oriented with the direction of the flow in the mixing channel.

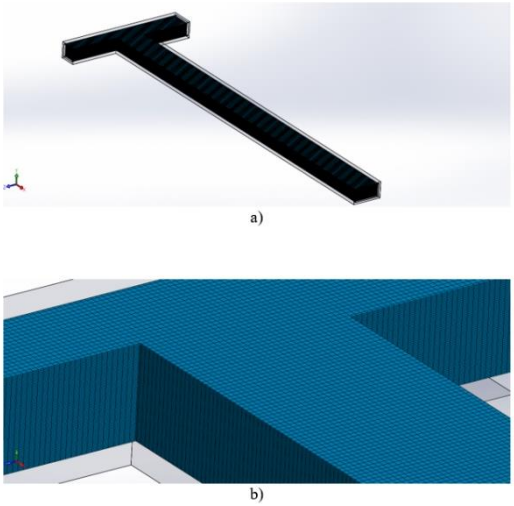

Figure 2 Computational mesh. a) General view. b) A close up view of the mixing zone of the A3 geometry

At the inlets Poiseuille-flow velocity profiles for rectangular cross sections [14] were

imposed and combined with the condition of species mass concentration of 1 in one of the inlets, and 0 in the opposite side. At the outlet, atmospheric pressure (1atm) was imposed, which presumes a fully developed flow. Additionally, impermeability and no-slip boundary conditions were imposed at the solid walls.

Twelve different pairs of flow rate values for the inlets were simulated for each geometry, corresponding to Reynolds numbers at the outlet channel ranging from 25 to 295.

The fluid defined for both inlets was water at 293K, which means that the fluids have the same properties. Notice that the different species concentrations imposed at the inlets are used to simulate the experimental conditions of using pure water in one inlet and a much diluted aqueous solution of bromothymol with the same physical properties at the opposing inlet.

3.3 Grid independence study

To study the independence of the results from the grid refinement, the starting point was the numerical simulation of the flow at the highest Reynolds number, 295, in the most asymmetrical geometry, A3, with a relatively course grid (1200 cells). Afterwards, refinements were done successively, until the solutions obtained belong to the asymptotic zone of convergence to the exact solution. Each refinement implies that a computational cell is subdivided into 8 cells, each one with half the dimensions of the original one. When the independent solution for this case was found, the same level of refinement was then used for all other geometries and simulations.

As the grid is refined, the numerical values of a given variable should tend asymptotically to the exact solution [15]. Therefore, an additional grid convergence study was also performed to confirm the spatial convergence of the numerical simulations. Since the cells are not cubic, the characteristic length h considered for the grid spacing was $h = \sqrt[3]{V_{cell}}$, with V_{cell} being the volume of a cell. For this study, the dependent variable used was α_{mix}, a global parameter standing for the mixing quality inside the micromixer. Five simulations with different h values were performed – see table 3. The order of grid convergence is defined as [15], with C being a constant, p the order of convergence and *H.O.T.* standing for higher order terms. A value of 2 for the order of convergence is generally acceptable [22].

$$E = f(h) - f_{exact} = Ch^p + H.O.T. \quad (7)$$

Neglecting the higher-order terms in equation (7) and applying the logarithm yields [15]:

$$\log(E) = \log(C) + p\log(h) \quad (8)$$

From equation (7), one can observe that p corresponds the slope of the straight line $\log(E)$ versus $\log(h)$, E being defined as: $E = \alpha_i - \alpha_{exact}$,

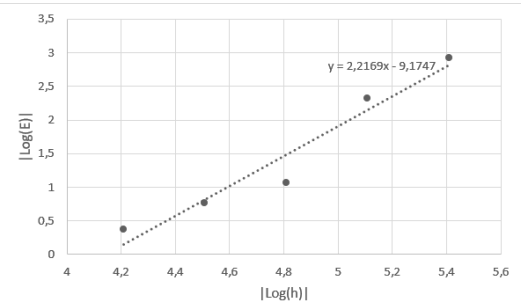

Figure 3 Plot of Log(E) versus Log(h). Modules have been taken because E and h are lower than one.

and $\log(C)$ being the origin intercept. Figure 3 shows the linear fitting of the results for the 5 used values of h. From that figure, the value estimated for p is 2.2, which means that one has a second order convergence scheme and, therefore, the numerical solution has a good rate of convergence.

4.Results and Discussion

One advantage of using CFD over experimental techniques commonly used in microfluidics is the possibility of identifying in detail the physical structures governing the flow inside microdevices like T-shaped micromixers, which are particularly relevant to explain the mixing effects between the incoming streams are concerned. In the present work, the symmetrical T-micromixer, which has been frequently studied experimentally by other authors [7,8], will be used as the reference case to validate the models used. Then, the flows inside assymetrical micromixers are analysed and the influence of increasing the levels of geometrical assymetry and the incoming flow rates on the degree of mixing is discussed.

As already mentioned, the parameter used to evaluate the micromixers performance is α_{mix}. This parameter has been widely used in the literature [2,6,8,14] as it allows for an effective comparison of different authors' results. Herein, α_{mix} is evaluated bidimensionally with 1300 concentration values obtained at the grid nodes at the cross-section of the mixing channel located at 1057μm away from the common wall of the two inlets.

Figure 4 synthetises the results of the present work by displaying all the values of α_{mix} that were obtained for the different flow simulations performed. This figure constitutes the departing point for the discussion presented in the next sections.

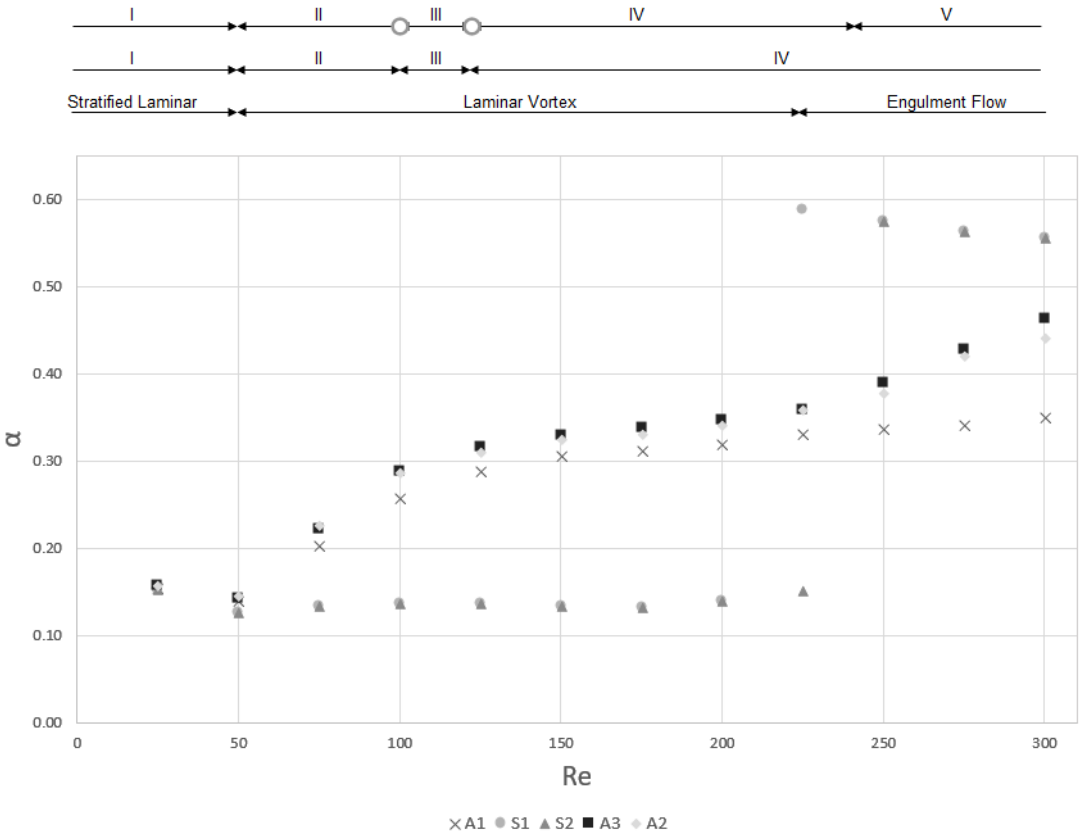

Figure 4 Mixing quality α_{mix} as a function of the Reynolds number (Re) for the mixers S1 (circle), S2 (triangle), A1 (cross), A2 (diamond) and A3 (square).

4.1 The Symmetrical Micromixer

For the flows in T-micromixers with symmetrical inlets (S1 and S2), it is possible to clearly identify 3 flow regimes in figure 4, similarly to that reported by other authors [2,5,6]. Moreover, figure 5 shows typical flow patterns for the different flow regimes in symmetrical micromixers.

Up to Re ≈ 50 (figure 4) the so-called stratified regime prevails. As it can be seen from figure 5a, this stratified regime is characterised by a segregated flow with straight parallel streamlines in the mixing channel, with little, or no advection in the mixing process. The only mixing mechanism acting is molecular diffusion. For this regime, the mixing quality is quite poor and decreases with increasing Re as residence time of the fluid particles inside de mixing channel decrease [5,6].

From Re ≈ 50 onwards the three-dimensional effects together with the centrifugal force experienced by the fluids in the T-junction region become important, and the flow is in the so-called vortex regime (figure 4). This regime is characterized by the appearance of two large and slow counter-rotating axial vortices at each stream in the T-junction region (parallel to the axis of the mixing channel). These four vortices do not promote mixing and dissipate downstream due to viscous forces [16]. On the other hand, two other small vortices (with strong rotation) form next to the wall common to both streams – see figure 5b. The symmetry of the micromixer promotes the cancelling of the momentum transported by each inlet fluid stream (one can imagine the fluids interface as a wall), inducing the conversion of kinetic energy into pressure energy. This increase of

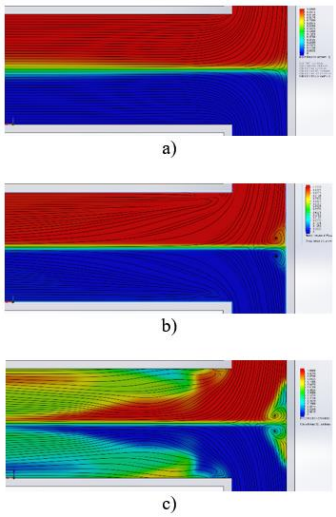

Figure 5 Concentration plots form the three regimes for symmetrical micromixers. a) Straight Laminar, b) Laminar Vortex and c) Engulfment Regime

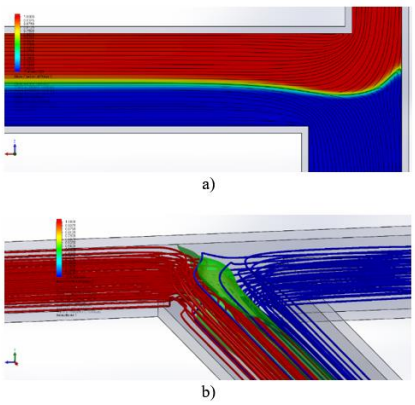

Figure 6 Flow visualizations of micromixer A3 at Re ≈ 75. a) represents a concentration plot and b) shows stream tubes.

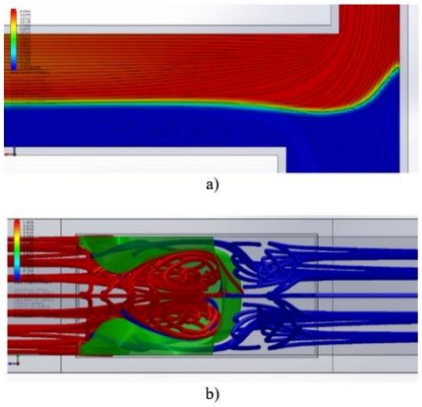

Figure 7 Flow visualizations of micromixer A3 at Re ≈ 125. a) represents a concentration plot and b) shows stream tubes in the mixing channel.

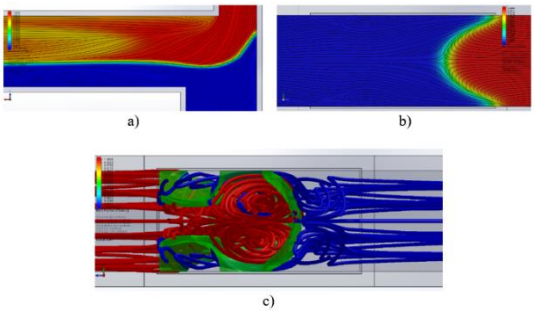

Figure 8 Flow visualizations of micromixer A3 at Re ≈ 200. a) represents a concentration plot, b) represents a concentration plot in the vicinity of the common wall, in the mixing zone and c) shows stream tubes in the mixing channel.

pressure in the mixing zone creates a local adverse pressure gradient that is responsible for the appearance of such vortex structures. Molecular diffusion still prevails, however, as the dominating mixing mechanism.

At Re ≈ 225 (figure 4, micromixer S1) the fluids interface breaks up, and the flow enters the engulfment regime – see figure 5c that illustrates the incursion of portions of each fluid stream into the other fluid flow. The two pairs of vortices of the previous regime degenerate into two larger vortices that promote mixing. Moreover, the two adjacent vortices located ate the common inlet wall also promote mixing by advection. One can easily observe in figure 5c the absence of flow separation downstream the 90º corners. This phenomenon is likely to be associated to the conversion of kinetic energy into pressure energy in the mixing zone that makes pressure gradient favourable downstream it. This engulfment regime is characterized by a sudden increase in mixing quality, due to the prevailing role of advection promoted by the mentioned flow structures in the mixing zone, and the fluid lamellae downstream the mixing channel that induce short diffusion lengths.

A final remark on how geometrical imperfections in the manufactured microchannels may influence the results is due. A comparison in figure 4 between the results for micromixers S1 and S2 evidences that imposing round corners in the mixing zone of micromixer S2 delays the flow transition to the engulfment regime, which occurs only at Re of approximately 250. This may be explained by the smaller intensity of the pair of vortices induced by the centrifugal forces that delay the disruption of fluids interface.

4.2 The Asymmetrical Micromixers

For the sake of easiness and clarity, from now on the fluid entering the micromixer through the narrowest inlet will be refered to as *fluid1* , the other being to as *fluid2*.

4.2.1 Effect of the Reynolds number and flow regimes

Figure 4 evidences that the increase of the Reynolds number results in an increasingly better mixing quality, with α_{mix} growing throughout the entire range of the studied Re. For the symmetrical micromixer, it is possible to observe that there is a sudden transition to the flow engulfment regime (Re around 225 for micromixer S1) that is accompanied by a sharp increase of α_{mix}. It is unquestionable the superior performance of the asymmetrical micromixers in the Re range 75-225. However, the symmetrical micromixer performs better after the transition to the engulfment regime (Re above 225).

The five different flow regimes found out in a previous experimental work [8] and above-described, were also identified herein.

Regime I: At Re bellow 50 the flow is quite stratified and there is almost no advection in the outlet channel; this is denoted by the presence of an interface separating the fluids streams that exhibits a growing thickness with the distance to the mixing zone due mainly to the molecular diffusion. Moreover, a slight perturbation of the streams interface at the mixing zone can be observed, which is caused by the larger momentum of *fluid1* that pushes the flow towards the opposite side.

Regime II: For Re above 50, it is observable figure 4 that the mixing quality increases considerably. In spite of the apparent similarities of this flow with that of regime I (see the midplane flow pattern in figure 6a), its distinctive feature is the existence of portions of fluid coming from the larger side that pass to the opposite side at the upper and lower planes. The amplification of the perturbation in the fluids interface caused by the different momenta of *fluid1* and *fluid2* is the major responsible for this phenomenon to occur. In fact, some *fluid2* elements divert to the upper and lower planes of the micromixer (see figure 6b). Additionally, the shape of the interface in the

mixing zone drives *fluid2* particles towards to the mixing chamber. In fact, in the mixing zone, the interface is slightly shifted to the largest inlet side due to the highest kinetic energy and momentum transported by *fluid1*. This fact also contributes for the diversion of *fluid2* to the upper and lower planes of the micromixer. This advective process appearance, with some entanglement of the stream tubes entering through different inlets clearly observable in figure 6b, promotes the fluids mixing improvement. Even though, the dominant mechanism of mixing appears to be still diffusion, but now with advection also playing a role.

Regime III: From figure 4, one can see that from Re ≈100 onwards there is a new flow regime. The first observable distinctive feature is the existence of a recirculation zone near the *fluid1*-side wall at the corner vicinity (see figure 7a that displays a horizontal midplane view of the flow pattern), that promotes the mixing of *fluid2* flowing nearby to with the fluid trapped in it, improving this way the micromixers performance. Moreover, the interface separating both fluids is now substantially deformed, as depicted in figure 7b, being able to drive some *fluid2* into its side of the mixing channel, and another fraction into the *fluid1*-side (by the upper and lower sides) and, therefore, promoting mixing through advection. The resulted twisted stream tubes straighten up further downstream in the outlet channel, but the fluids lamellae generated in the mixing zone allow for improving mixing quality Also, it is possible to observe in figure 8b the appearance of two counter-rotating vortices, formed by the action of the centrifugal force acting on *fluid1* portions flowing in the upper and lower parts of the channel, which makes them to be deflected towards the centre and side wall of the mixing channel. Downstream the mixing zone, the flow pattern appears to lose symmetry (figure 7a), which is due to the deficit of *fluid2* momentum when compared to that of *fluid1*. In the T-junction zone, advection is the dominant mixing mechanism, and the fluids interface is no longer well defined.

Regime IV: Figure 8a shows mixing already occurring at the horizontal midplane inside the recirculation zone (which is significantly bigger than in the previous case) on the *fluid1* side. The most distinctive feature of this flow regime (Re above 150 in figure 4) is the appearance above this midplane, at the upper part of the mixer next to the wall common to both inlet channels, of a new counter-rotating vortex pair in the *fluid2*-side (figure 9b, in the left side). This pair of vortices has a great influence on the performance of the micromixer as it helps directing the flow of *fluid2* towards the mixing channel and limits the amount that goes to the *fluid1* side. In the mixing channel, the streamlines straighten up and vortices end up dissipating, so diffusion becomes the dominant

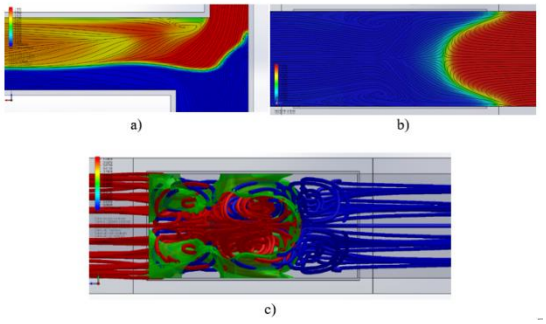

Figure 9 Flow visualizations of micromixer A3 at Re ≈ 275. a) represents a concentration plot, b) represents a concentration plot in the vicinity of the common wall, in the mixing zone and b) shows stream tubes in the mixing channel.

mixing mechanism. On the other hand, advection is strong in the mixing zone. Moreover, as the flow rates increase, more *fluid2* penetrates into the *fluid1*-flow side and this flow engulfs even more the *fluid2*, intensifying the pair of vortices already existent in regime III due to higher velocities and, consequently, higher centrifugal forces.

Regime V: Transition to regime V (Re above 225 in figure 4) occurs when the pair of vortices present near the wall common to both inlets merge into a single vortex, now visible in the midplane of the micromixer (see figure 9a), but shifted towards the fluids interface. Because of that, the flow is no longer directed towards the mixing channel, going straight to the *fluid1*-side. As *fluid1* elements transport more momentum and kinetic energy, *fluid2* elements, besides being accelerated due to the local constriction generated by the vortices presence, are also deviated towards the upper and lower sides of the mixing channel. Additionally, the pair of vortices formed in the *fluid2*-side, near the common wall (see figure 9b) intensify their strength. This promotes better mixing, denoted by the more sharp increase of α_{mix}, as shown in figure 4 (micromixers A3 and A2). As a consequence of these new flow structures, the velocity field becomes strong enough for the fluids interface to be completely disrupted (see figure 9c).

4.2.2. Effect of the Degree of Asymmetry

It is also clear from figure 4 that the symmetrical micromixers exhibit a better performance than the asymmetrical ones for equal Re whenever the former attain the engulfment regime. This is due to the higher pressure attained in the T-junction region for the symmetrical case due to the more efficient deceleration of the incoming streams (conversion of kinetical energy into pressure energy). This higher pressure level in the symmetrical case generates an adverse pressure gradient for the inlet flows responsible for the recirculation zones appearing in the inlet channels near the wall common to both inlets, and generates an intense favourable pressure gradient for the

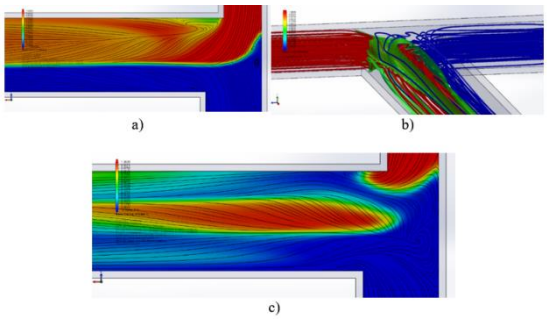

Figure 10 Flow visualizations of micromixer A1 at Re ≈ 275. a) show a concentration plot of the micromixer at the middle plane, b) represents a three dimensional view of the mixing zone with stream tubes and c) shows a concentration plot of the micromixer at a plane 40μm above the middle one.

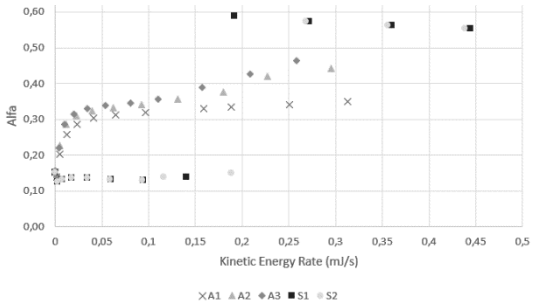

Figure 11 Plot of the mixing quality versus the kinetic energy rate at the micromixer inlets for the mixer A1 (cross), A2 (triangle), A3 (diamond), S1 (square), S2 (circle).

outlet channel flow responsible for the very strong attenuation of the recirculation zones immediately after the corners (compare figure 5c with figures 9a,b). This is probably the reason why the mixing quality decreases whit the increase of Re in the engulfment regime within symmetrical micromixers.

Figure 4 also evidences that, as far as the asymmetrical micromixers are concerned, the larger is the degree of asymmetry of the micromixer, the better is its performance. This becomes increasingly pronounced at higher Reynolds numbers. This is most probably due to the dominating viscous forces at the lowest Reynolds numbers in the momentum balance; such predominant viscous forces damp potential flow perturbations that arise from geometrical differences. This reinforces the matching between regime I for asymmetrical micromixers and the stratified regime for the symmetrical micromixers.

As the Reynolds number increases and inertial forces become increasingly important, the level of asymmetry becomes also a most influencing parameter concerning the mixing quality. Most physical structures discussed in the previous section form because there is a difference in the momentum carried by fluid elements from both inlet streams.

To reinforce the previous reasoning, a new dependent variable of the quality mixing (α_{mix}) variation, the total kinetic energy rate at the inlet streams (I_{KE}), is proposed – see equation (2). The results are presented in figure 10 and confirm the different behaviours between the symmetrical and asymmetrical micromixers above-discussed.

Moreover, those results also evidence that, for the same Re, the symmetrical geometries exhibit always larger values of the total kinetic energy rate (as, according to equation (2), this parameter scales with v^3) than the corresponding asymmetrical cases. This total kinetic energy rate is therefore more representative of the actual flows effects. In fact, higher total kinetic energy rate values help sustai ning the presence of vortices (in the vortex regime) and this reinforces the justification for the lack of increase of the mixing quality observable in figure 10, as such flow structures are not favourable to the mixing process.

The previous tendency is also observable for asymmetric micromixers: less asymmetrical micromixers (A1) exhibit higher values of total inlet kinetic energy rate for the same Re at the outlet channel. This trend is also related to the more intense velocity field present at the inlets of micromixer A1, due to its lower width relative to A3. Looking from this point of view, and for the same Re in the mixing channel, as a lower asymmetry results in a higher kinetic energy rate, and inferior mixing quality, one can infer that the kinetic energy rate transported by the fluid elements represent a source of energy that helps sustaining the existence of the vortices present in the mixing zone, which do not favour mixing.

Figure 10 shows the flow visualization inside the micromixer A1 (the least asymmetrical) at Re ≈ 275 (regime IV). Figure 11b confirms that the flow is more segregated than that at micromixer A3 (compare with figure 9c), as it is no longer possible to detect a strong entanglement of the more intense vortices from both fluids and there is practically no *fluid2* diverted to the side of *fluid 1*. Figures 11a and c, clarify the reason behind this poorer performance of micromixer A1 (when compared to A3). For micromixer A1, the pair of vortices that were present near the common wall of both inlets at Re ≈ 200 now merged into a single one (similarly to micromixer A3 in regime V). This vortex occupies the whole height of the geometry and directs more *fluid2* to its side in the mixing channel, and the amount that manages to penetrate into the *fluid1*-side is not enough to disrupt the interface, which makes the flow to be kept in regime IV. This is in opposition to that occurring in micromixer A3, where the corresponding single vortex in regime V occupied only the vicinity of the midplane (and was located close to the fluids interface, allowing the formation of another pair of vortices parallel to the axis of the mixing channel).

Summing up, the main differences when comparing to the least to the most asymmetrical

micromixers are related to the non-disruption of the fluids interface in the former and, because of that, downstream the mixing zone advection is still not strong enough and the characteristic lengths are not small enough for diffusion to occur efficiently when the vortices dissipate, and the streamlines straighten. In the more asymmetrical micromixers, as seen before, the complete disruption of the fluids interface resulted in a significant increase in the advection mechanisms.

5. Conclusions

Comparison between the geometry with perfect ninety-degree corners and the one with smoothed out corners shows that geometrical imperfections delay the transition to the engulfment regime, which agrees with the experimental tests.

For the asymmetrical micromixers, the numerical simulations allowed for the clear and detailed identification, and characterization, of five different regimes as the Reynolds number at the outlet channel increases.

In terms of geometry, results show that the more asymmetrical the micromixer is, the better is the performance (*i.e.* the larger is the mixing parameter). The Kinetic Energy Rate proved a useful tool to understand the role of the degree of asymmetry in the performance of the micromixers.

As conclusion, the initial objectives can be considered as accomplished. The results show a high consistency with the ones obtained in the experimental works in which the present one is based on, and allowed a detailed characterization of the flow inside asymmetrical T-micromixers, with identification of the physical mechanisms and structures involved, and how they are influenced by variations in mass flow rate and degree of asymmetry. Therefore, one may consider that the gap in the knowledge left by the previous experimental works was filled.

References

[1] Dreher S, Kockmann N, Woias P. Characterization of laminar transient flow regimes and mixing in T-shaped micromixers. Heat Transfer Engineering 2009;30(1–2):91–100. doi:10.1080/01457630802293480

[2] Mansur EA, Ye M, Wang Y, Dai Y. A state-of-the-art review of mixing in microfluidic mixers. Chinese Journal of Chemical Engineering 2008;16(4):503-516. doi:10.1016/s1004-9541(08)60114-7

[3] Bothe D, Stemich C, Warnecke HJ. Fluid mixing in a T-shaped micro-mixer. Chemical Engineering Science 2006 61:2950 – 2958. doi:10.1016/j.ces.2005.10.060

[4] Basavarajappa M. Experimental investigation and characterization of mixing in a T-channel mixer for asymmetric inlet conditions. PhD thesis. The University of Utah. 2012

[5] Capretto L, Cheng W, Hill M, Zhang X. Micromixing within microfluidic devices. Topics Current Chemistry 2011;304:27–68. doi:10.1007/128_2011_150

[6] Engler M, Kockmann N, Kiefer T, Woias P. Numerical and experimental investigations on liquid mixing in static micromixers. Chemical Engineering Journal 2004;101:315–322. doi:10.1016/j.cej.2003.10.017

[7] Silva JP, dos Santos A, Semiao V. Experimental characterization of pulsed Newtonian fluid flows inside T-shaped micromixers with variable inlets widths. Experimental Thermal and Fluid Science 2017;89:249–258. doi:10.1016/j.expthermflusci.2017.08.01

[8] Calado B, dos Santos A, Semiao V. Characterization of the mixing regimes of Newtonian fluid flows in asymmetrical T-shaped micromixers. Experimental Thermal and Fluid Science 2016;72:218–227. doi:10.1016/j.expthermflusci.2015.11.010

[9] S. Hardt and F. Schönfeld. Microfluidic Technologies for Miniaturized Analysis Systems. Springer Science & Business Media, 2007

[10] Hoffmann M, Schlüter M, Räbiger N. Experimental investigation of liquid–liquid mixing in T-shaped micro-mixers using μ-LIF and μ-PIV. Chemical Engineering Science 2006;61:2968 – 2976. doi:10.1016/j.ces.2005.11.029

[11] Wong SH, Ward MCL, Wharton CW. Micro T-mixer as a rapid mixing micromixer. Sensors and Actuators B 2004;100:359-379. doi:10.1016/j.snb.2004.02.008
doi:10.1016/j.icheatmasstransfer.2010.01.012

[12] Hirsch C. Numerical Computation of Internal and External Flows. Volume 1 - Fundamentals of Computational Fluid Dynamics. 2nd ed. Oxford, England:Butterworth-Heinemann; 2007

[13] Patankar SV. Numerical heat transfer and fluid flow. USA: Hemisphere Publishing Corporation; 1980

[14] Bruus H. Theoretical microfluidics - Lecture notes. 2nd ed. Autor's Edition. 2005

[15] Roache PJ. Verification and validation in computational science and engineering. Albuquerque, New Mexico: Hermosa Publishers, 1998

[16] Kockmann N, Engler M, Föll C, Woias P Liquid mixing in static micro mixers with various cross sections. 1st International Conference on Microchannels and Minichannels:911-918, 2003. doi:10.1115/icmm2003-1121